

NACA TN 3616 9066



NATIONAL ADVISORY COMMITTEE FOR AERONAUTICS

TECHNICAL NOTE 3616

CHARTS FOR ESTIMATING ROTOR-BLADE FLAPPING MOTION
OF HIGH-PERFORMANCE HELICOPTERS

By Robert J. Tapscott and Alfred Gessow

Langley Aeronautical Laboratory
Langley Field, Va.



Washington
March 1956

AFMDC

TECHNICAL REPORT



TECHNICAL NOTE 3616

CHARTS FOR ESTIMATING ROTOR-BLADE FLAPPING MOTION
OF HIGH-PERFORMANCE HELICOPTERS

By Robert J. Tapscott and Alfred Gessow

SUMMARY

Theoretically derived charts showing steady-state and first- and second-harmonic flapping coefficients are presented for helicopter rotors having hinged rectangular blades with a linear twist of 0° , -8° , and -16° . The charts, showing the rotor flapping coefficients for combinations of inflow ratio and blade pitch angle, are presented for tip-speed ratios ranging from 0.05 to 0.50.

The theory on which the charts are based does not contain any small-angle assumptions regarding blade-section inflow angles and velocities. These charts are therefore considered applicable, within the limits discussed, for flight conditions involving high inflow velocities and large regions of reversed velocity. Other than including an approximate allowance for stall in the reversed-velocity region, the charts do not include stall or compressibility effects.

INTRODUCTION

A knowledge of the steady-state flapping behavior of lifting rotors is useful in the design of helicopter hubs and control systems, in estimating rotor-fuselage clearances, and as a prerequisite to the numerical (that is, step-by-step integration) evaluation of the aerodynamic characteristics of rotors. Equations for calculating rotor-blade flapping are available from various theories; however, in order to reduce computations to a minimum, this paper presents charts whereby theoretical flapping values can be obtained directly.

The charts were prepared from the extended rotor theory of reference 1. Since the equations of reference 1 do not assume the rotor inflow angle or the rotor angle of attack to be small, they can be used in calculating rotor-blade flapping over a wide range of operating conditions. The assumption is made, however, that, outside the reversed-velocity region, the section angles of attack are small; therefore, these

angles can be replaced by their sines. Also, with the exception of an approximate allowance for stall in the reversed-velocity region, the theory and, thus, the charts of this paper do not include stall or compressibility effects. The charts were calculated for hinged blades having 0° , -8° , and -16° of twist and for a range of conventional values of blade mass constant.

SYMBOLS

β	blade flapping angle at particular azimuth position measured from plane perpendicular to axis of no feathering, radians or deg
a_0	constant term in Fourier series that expressed β ; hence, rotor coning angle
a_n	coefficient of $\cos n\psi$ in Fourier series that expresses β
b_n	coefficient of $\sin n\psi$ in Fourier series that expresses β
γ	mass constant of rotor blade; expresses ratio of air forces to mass forces $c_p a R^4 / I_h$
μ	tip-speed ratio, $\frac{V \cos \alpha}{\Omega R}$
λ	inflow ratio, $\frac{V \sin \alpha - v}{\Omega R}$
θ_1	difference between blade-root and blade-tip pitch angles, positive when tip angle is larger, deg
θ_0	blade-section pitch angle at blade root, deg
$\theta_{.75}$	blade-section pitch angle at 0.75 radius; angle between line of zero lift of blade section and plane perpendicular to axis of no feathering, deg
$\alpha_{(1.0)}(270^\circ)$	blade-element angle of attack at tip of retreating blade at 270° azimuth position, deg
$\alpha_{(u_T=0.4)}(270^\circ)$	blade-element angle of attack at radius at which tangential velocity equals 0.4 tip speed at 270° azimuth position, deg

V	velocity of helicopter along flight path, fps
α	rotor angle of attack; angle between axis of no feathering (that is, axis about which there is no cyclic-pitch change) and plane perpendicular to flight path; positive when axis is inclined rearward, deg
α_r	blade-element angle of attack, measured from line of zero lift, radians
v	induced velocity at rotor (always positive), fps
r	radial distance from center of rotation to blade element, ft
Ω	rotor angular velocity, radians/sec
R	blade radius measured from center of rotation, ft
ρ	mass density of air, slugs/cu ft
a	slope of curve of section lift coefficient against section angle of attack in radians (assumed equal herein to 5.73)
I_h	mass moment of inertia of blade about flapping hinge, slug-ft ²
ψ	blade azimuth angle measured from downwind position in direction of rotation, deg
c	blade-section chord, ft
u_T	nondimensional component of resultant velocity at blade element

METHOD OF ANALYSIS

The analysis of reference 1 was developed for linearly twisted rectangular blades with the flapping hinge located on the rotor center and perpendicular to the rotor axis and to the blade span. All velocities, angles, forces, and moments are referred to the axis of no feathering. An explanation of this system of axes, together with means for applying the equations based on this system to pure feathering or combination

flapping-feathering configurations, is given in reference 2. Configurations involving offset or tilting of the flapping hinges can be evaluated by the numerical method presented in reference 3, which can also be used to compute flapping motion in flight conditions outside the range of the analytical theory.

As used herein, blade flapping is the angle between the blade-span axis and a plane perpendicular to the axis of no feathering. Since, in the theory, the blade is considered inflexible, the calculated flapping angle should be considered to represent the angle between the plane of no feathering and a line through the flapping hinge and the 0.75-radius station of the blade. The flapping angle is expressed as a function of the azimuth angle by means of a Fourier series expansion that can be terminated for most purposes after the second harmonic. The expression for the flapping angle is then

$$\beta = a_0 - a_1 \cos \psi - b_1 \sin \psi - a_2 \cos 2\psi - b_2 \sin 2\psi$$

The coefficients are related in reference 1 by means of five simultaneous equations expressed as functions of tip-speed ratio μ , inflow ratio λ , pitch angle θ_0 , blade twist θ_1 , and airfoil-section characteristics. The specific values of these variables that were used in the present paper in preparing the charts for rotor flapping coefficients correspond to the values represented in the performance charts of references 4 and 5; the five simultaneous equations were solved for the same range of variables.

DESCRIPTION OF CHARTS

The rotor coning angle a_0 and the first-harmonic flapping coefficients a_1 and b_1 are presented in figure 1 as a function of λ and $\theta_{.75}$ for tip-speed ratios ranging from 0.05 to 0.50 and for blade twists of 0° , -8° , and -16° . In the figure, a_0 and b_1 are divided by the blade mass constant γ ; thus, all the coefficients are essentially independent of γ .

As in any theoretical calculation that does not make allowance for blade stall, it is desirable to include limit lines on the plots to indicate the flight conditions at which the theory is expected to become inaccurate as a result of stall and, at the same time, to indicate limiting conditions of operation. Such limit lines are included in the performance charts of references 4 and 5, for example, and can be used in conjunction with the flapping charts of this paper. For the sake of convenience, however, the inboard and outboard limit lines of references 4 and 5 are included in figure 1. Also, to avoid crowding of the lines,

the limit lines for each of the twist values are shown on separate plots; the limit lines apply to 0° twist on the a_0/γ plots, to -8° twist on the a_1 plots, and to -16° twist on the b_1/γ plots. The limit lines corresponding to a particular twist that appear on one plot can be applied to the other plots at a given tip-speed ratio by simply matching the corresponding values of λ and $\theta.75$.

The second-harmonic flapping coefficients are presented in figure 2 for values of tip-speed ratio of 0.30, 0.40, and 0.50 for $\theta_1 = -8^\circ$. Values of the coefficients for tip-speed ratios less than 0.30 are not given because the magnitude of the coefficients for the lower tip-speed ratios is less than half a degree, which is considered to be within the accuracy of the theory. Also, second-harmonic flapping coefficients for 0° and -16° of twist are omitted because they differed by a negligible amount from the values shown for -8° . Because the blade mass constant cannot be factored out for the second-harmonic flapping coefficients as it can for the first-harmonic coefficients, figure 2 contains separate plots for $\gamma = 15$, $\gamma = 9$, and $\gamma = 3$.

The charts of figures 1 and 2 can be used directly to yield flapping coefficients if λ , $\theta.75$, and μ are known at the start. If, as more often is the case, the known starting quantities are tip-speed ratio, thrust coefficient, and power, then the corresponding values of pitch angle and inflow ratio can be obtained from the charts of references 4 and 5.

It will be noted that the effects of twist on blade flapping are small and that the differences shown are probably within the accuracy of the calculations.

APPLICABILITY OF CHARTS

The usefulness of the charts in different applications wherein an estimation of blade flapping is required is, of course, dependent on the assumptions and limitations of the theory on which the charts are based. These limitations and the extent to which they affect the usefulness of the charts are discussed in the following sections.

Assumptions and Limitations

The extended theory from which the charts presented herein were derived (ref. 1) does not contain any small-angle assumptions regarding blade-section inflow angles and velocities. The assumption is made, however, that outside the reversed-velocity region the section angle of

attack α_r is small and can be replaced by $\sin \alpha_r$. Even with $\alpha_r = 20^\circ$, this assumption causes only about a 2-percent difference in the numerical value of the angle. For these reasons, it is believed that the charts are applicable for cases wherein the rotor inflow velocity is relatively large, such as might occur with high-performance helicopters flying at high forward speeds or at high rates of climb.

It has been demonstrated (see ref. 2, for example) that, for flight conditions which do not involve appreciable stall or compressibility effects, analytical rotor theory similar to that used in preparing figures 1 and 2 can predict the coning angle and the longitudinal and lateral flapping angles within about 1° . In order to achieve this accuracy in predicting b_1 , however, it was necessary to assume a longitudinal variation, instead of a uniform distribution, of induced velocity over the rotor disk. Inasmuch as the theory on which the present charts are based assumes uniform inflow, it is expected that the accuracy of the values of b_1 given in figure 1 would be improved by applying a correction for nonuniform inflow. The correction to b_1 for nonuniform inflow given in reference 6 would be sufficiently accurate for most purposes.

The charts presented herein were calculated for rotors having uniform chord blades and zero flapping-hinge offset. In addition, although the coefficients a_0 and b_1 are divided by the mass constant, a fixed value was used in the calculation of these coefficients. This procedure does not eliminate the higher order effects of mass constant on these coefficients (a_0 and b_1); however, subsequent checks indicated these higher order effects to be well within the accuracy of reading the charts. Thus, these charts, as were previous chart presentations of the theory of reference 1, are considered applicable for the conventional range of blade mass constants (approximately 0 to 25).

Satisfactory comparisons are indicated also between calculated blade motion and blade motion measured for blades having taper ratios (root chord divided by tip chord) as high as 3:1. In such cases, however, the taper ratio was accounted for theoretically by basing the rotor solidity and blade mass constant on an equivalent blade chord. For the determination of rotor solidity, the equivalent blade chord is defined as

$$\frac{\int_0^R cr^2 dr}{\int_0^R r^2 dr}$$
; whereas, for the determination of mass constant,
$$\frac{\int_0^R cr^3 dr}{\int_0^R r^3 dr}$$
 is considered to be more accurate.

The effect of flapping-hinge offset on blade motion appears to vary with both mass constant and tip-speed ratio. Calculations (ref. 7, for

example) show that these effects can be considerable. In the event that calculations are desired for cases with significant amounts of flapping-hinge offset (greater than 1 or 2 percent), the theory of reference 3 may be used. In this regard, the charts of this paper should prove useful in providing initial estimates for the iterative process, and thus considerably reduce the time required to obtain a solution.

Applicability to Seesaw Rotors

Although calculated for rotors having individually hinged blades, the charts presented herein are also useful in the case of seesaw rotors; for example, the longitudinal flapping coefficient a_1 is unaffected.

With regard to the coning angle a_0 , and thus the lateral coefficient b_1 , the validity of the value obtained from the charts presented herein will be dependent on the stiffness of the blade-hub combination relative to the stiffness imparted by the centrifugal forces due to rotation. For typical seesaw-rotor systems, the blade-hub stiffness appears to be about 8 percent, or less, of the stiffness imparted by the centrifugal forces; thus, the charts should give fair approximations for most purposes. In any case, the charts may be used to estimate the preset coning angle a_0 for the seesaw-rotor system. It should be noted again in this connection that the charts as derived represent the angle between the no-feathering plane and a line through the flapping hinge and the 0.75-radius station rather than a blade-root angle.

Stall and Compressibility Effects

As mentioned previously, the theory on which the charts of this paper are based does not make any allowance for blade stall or the variation of blade-section characteristics with Mach number. When the section angles of attack exceed the stall angle or when the Mach number for lift and drag divergence is exceeded, the charts are not expected to predict flapping coefficients accurately. Inasmuch as conditions for which representative blade-section angles of attack reach 12° and 16° are indicated on the charts, an estimate can be made of stall conditions of the rotor for given flight conditions. It is believed that the effects of moderate amounts of stall (tip angle at $\psi = 270^\circ$ exceeding the stall angle by as much as 4°) can be estimated by the trends indicated in reference 2. In cases where larger amounts of stall are present on the rotor or where a more extensive study of the effects of stall is desired, the method of reference 3 may be applied.

Unpublished calculations indicate that the effect of compressibility on blade motion is to bring about a general increase in the values of the

flapping coefficients. The largest increment is seen to occur in the longitudinal flapping coefficient a_1 ; the increment increases with Mach number to about 1° at a Mach number of 1 at the tip of the advancing blade. The changes in coning angle a_0 and lateral flapping coefficient b_1 are about equal, and amount to about one-half of that noted for a_1 . Such trends, although generally small, may become significant for some purposes and should be considered when the charts of this paper are used to predict blade flapping for cases in which compressibility effects may be present. In such cases, the effects of compressibility may be evaluated quantitatively by use of suitable airfoil characteristics in conjunction with the step-by-step method discussed in reference 3.

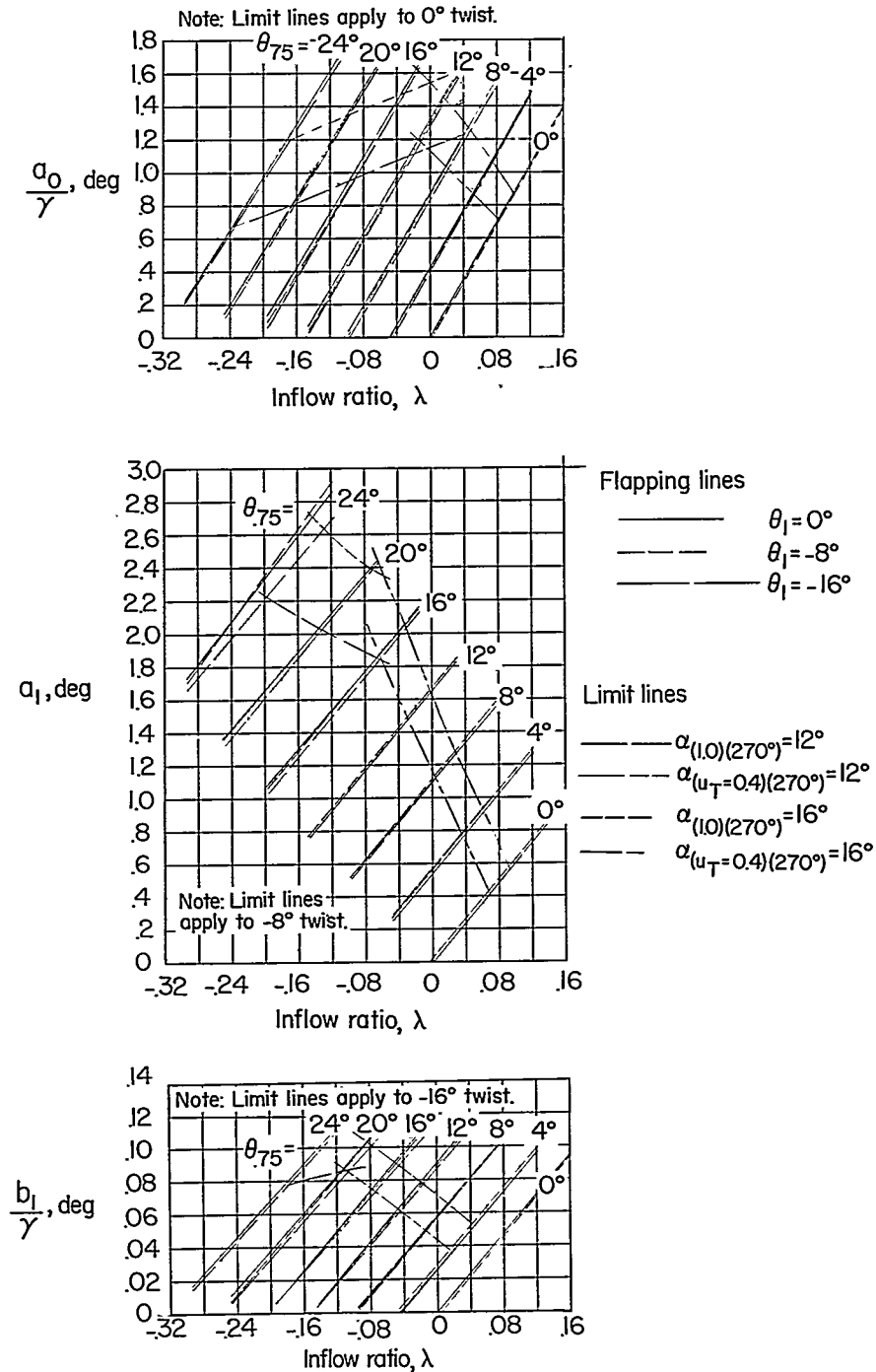
CONCLUDING REMARKS

Theoretically derived charts showing steady-state and first- and second-harmonic flapping coefficients have been presented for helicopter rotors having blades with a linear twist of 0° , -8° , and -16° . The charts, showing rotor flapping coefficients for combinations of inflow ratio and blade pitch angle, were presented for tip-speed ratios ranging from 0.05 to 0.50. Inasmuch as the theory on which the charts are based does not contain any small-angle assumptions regarding blade-section inflow angles and velocities, the charts are considered applicable, within the limits discussed, for flight conditions involving high inflow velocities and large regions of reversed velocity. Other than including an approximate allowance for stall in the reversed-velocity region, the charts do not include stall or compressibility effects.

Langley Aeronautical Laboratory,
National Advisory Committee for Aeronautics,
Langley Field, Va., October 31, 1955.

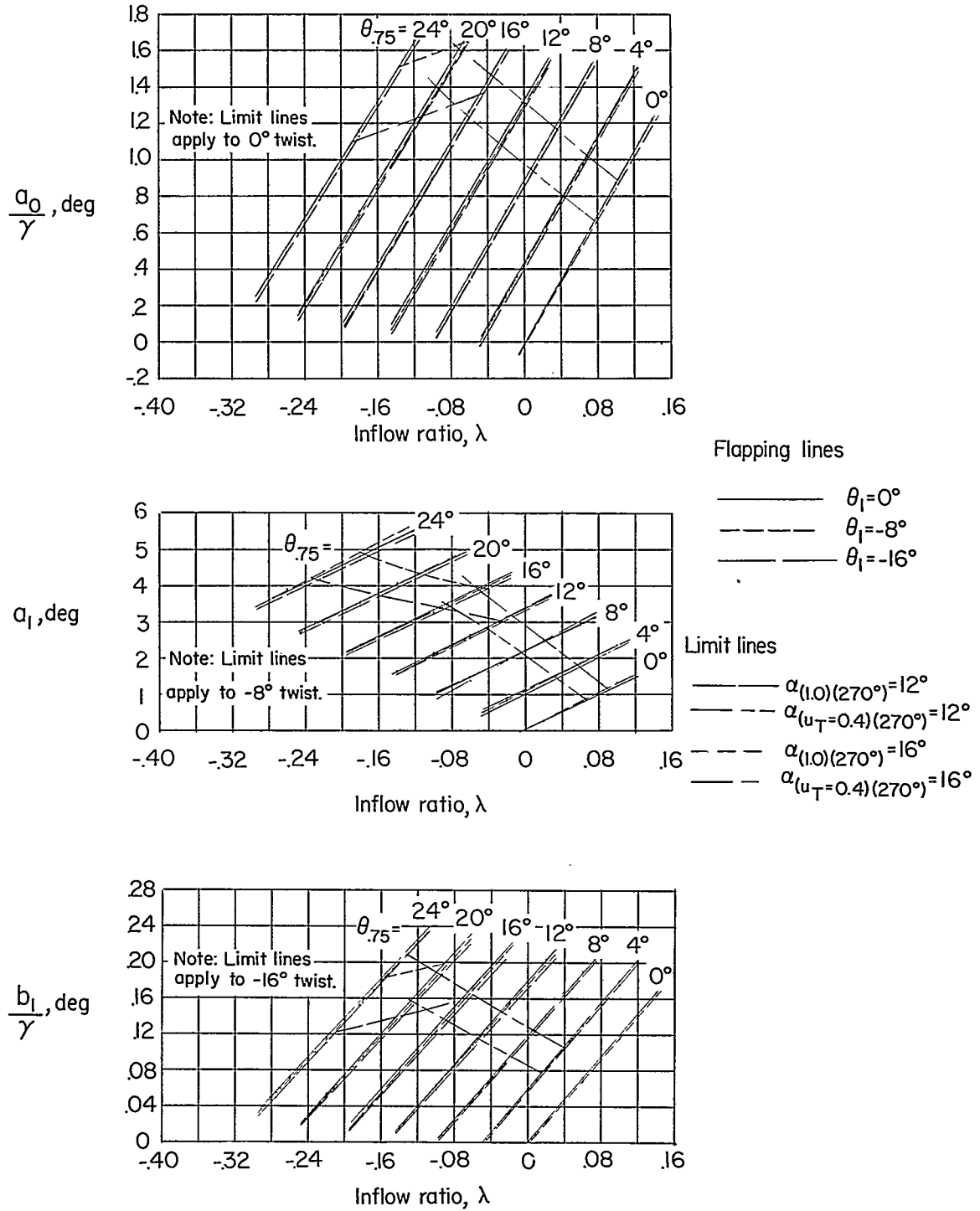
REFERENCES

1. Gessow, Alfred, and Crim, Almer D.: An Extension of Lifting Rotor Theory To Cover Operation at Large Angles of Attack and High Inflow Conditions. NACA TN 2665, 1952.
2. Myers, Garry C., Jr.: Flight Measurements of Helicopter Blade Motion With a Comparison Between Theoretical and Experimental Results. NACA TN 1266, 1947.
3. Gessow, Alfred, and Crim, Almer D.: A Method for Studying the Transient-Blade-Flapping Behavior of Lifting Rotors at Extreme Operating Conditions. NACA TN 3366, 1955.
4. Gessow, Alfred, and Tapscott, Robert J.: Charts for Estimating Performance of High-Performance Helicopters. NACA TN 3323, 1955.
5. Tapscott, Robert J., and Gessow, Alfred: Supplementary Charts for Estimating Performance of High-Performance Helicopters. NACA TN 3482, 1955.
6. Wheatley, John B.: An Aerodynamic Analysis of the Autogiro Rotor With a Comparison Between Calculated and Experimental Results. NACA Rep. 487, 1934.
7. Meyer, John R., Jr., and Falabella, Gaetano, Jr.: The Effect of Blade Mass Constant and Flapping Hinge Offset on Maximum Blade Angles of Attack at High Advance Ratios. Proc. Eighth Annual Forum, Am. Helicopter Soc., Inc., May 15-17, 1952, pp. 51-87.



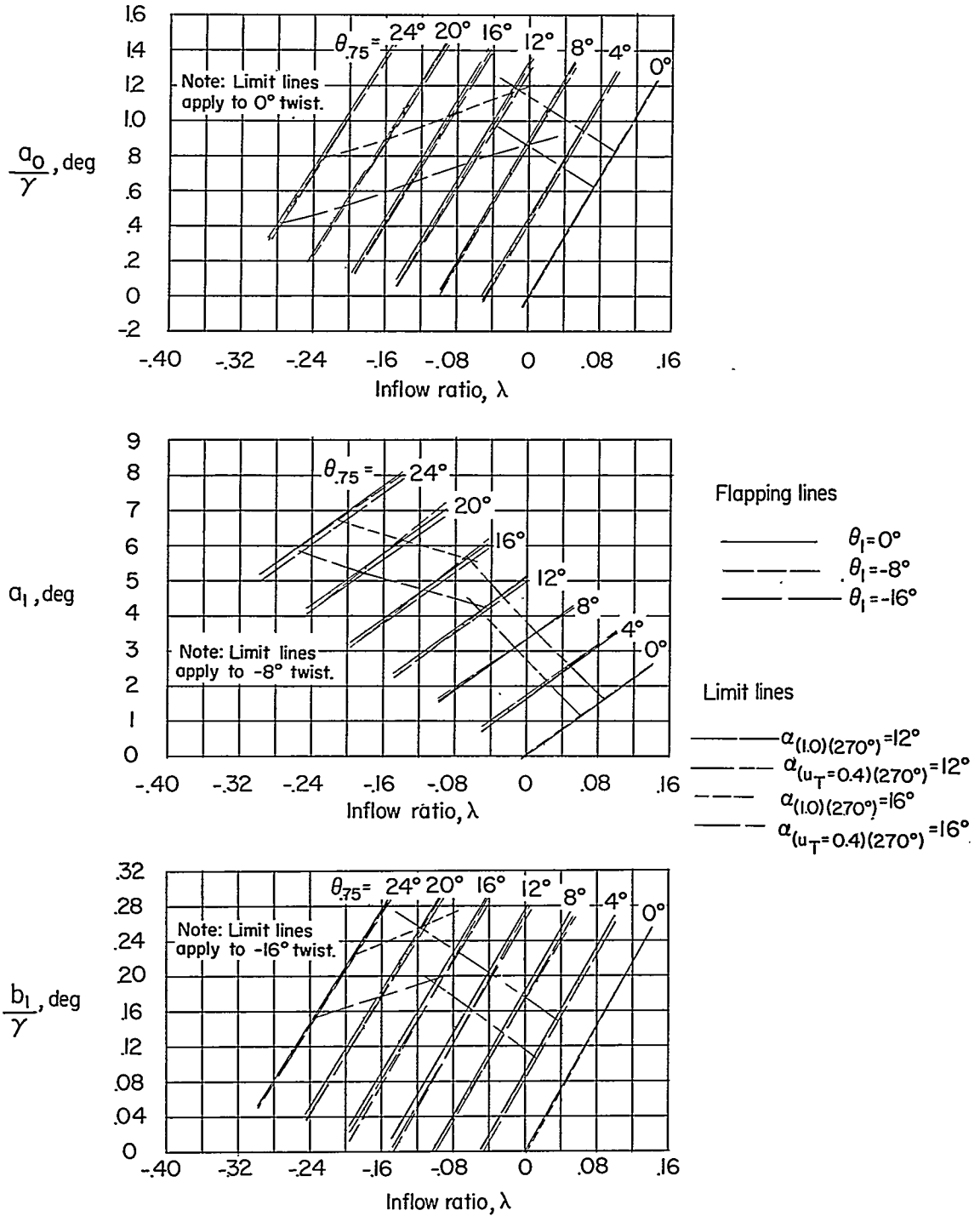
(a) $\mu = 0.05$.

Figure 1.- Rotor coning angle and first-harmonic flapping coefficients as a function of pitch angle and inflow ratio for blades having 0°, -8°, and -16° of twist.



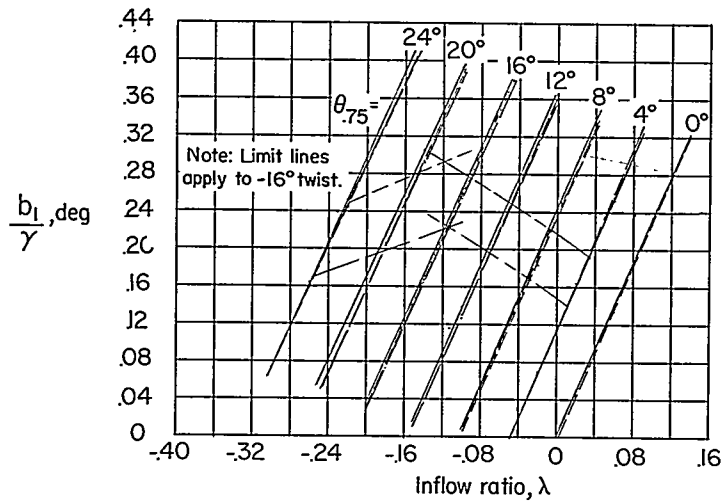
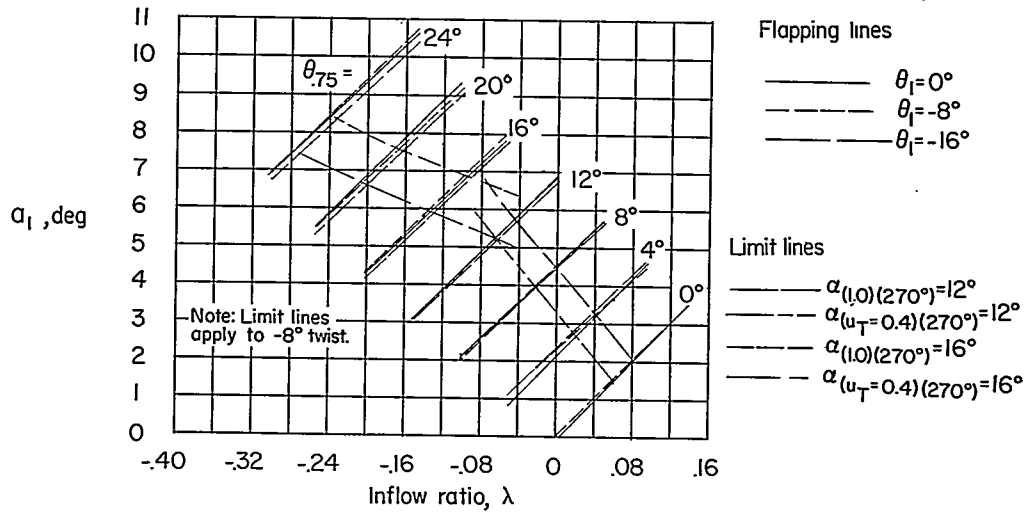
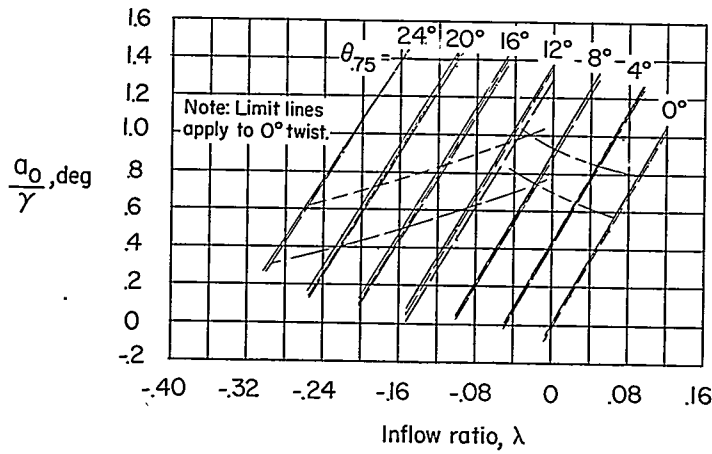
(b) $\mu = 0.10$.

Figure 1.- Continued.



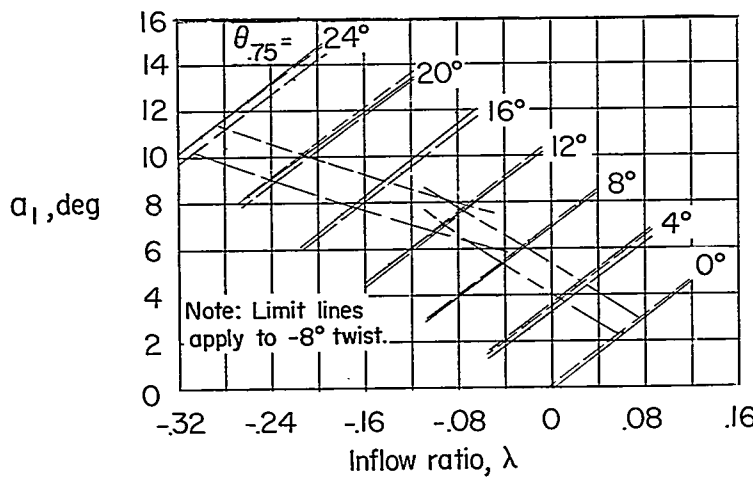
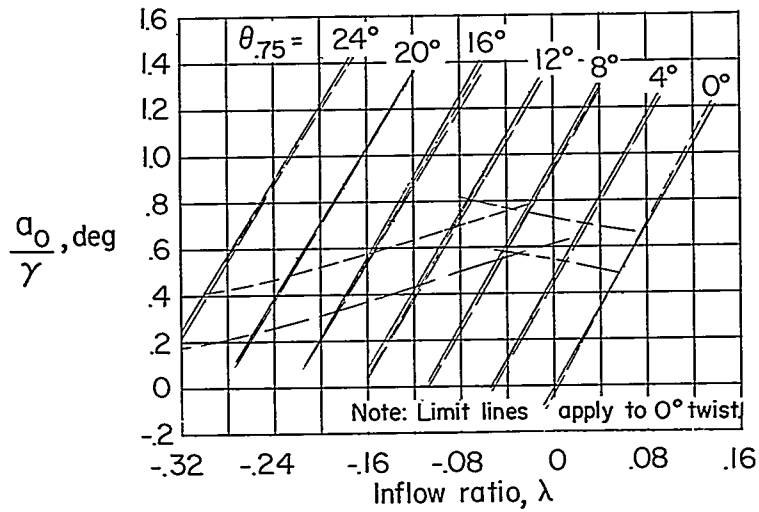
(c) $\mu = 0.15$.

Figure 1.- Continued.



(d) $\mu = 0.20$.

Figure 1.- Continued.

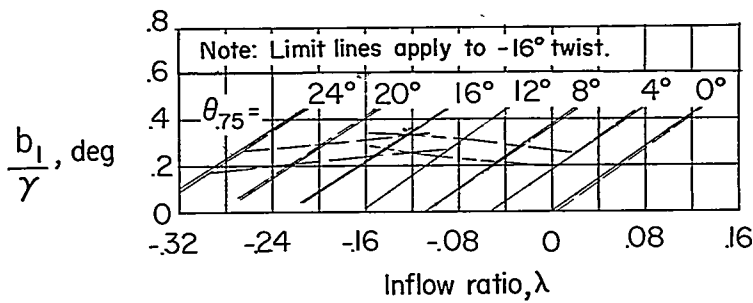


Flapping lines

- $\theta_1 = 0^\circ$
- $\theta_1 = -8^\circ$
- - - - $\theta_1 = -16^\circ$

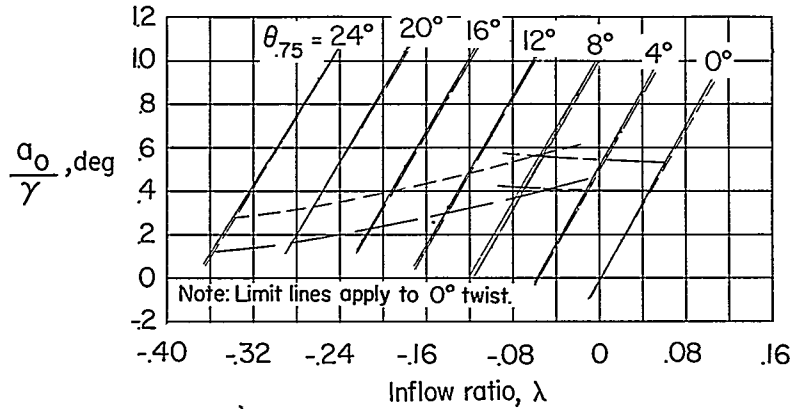
Limit lines

- $\alpha_{(1.0)}(270^\circ) = 12^\circ$
- $\alpha_{(u_T=0.4)}(270^\circ) = 12^\circ$
- - - - $\alpha_{(1.0)}(270^\circ) = 16^\circ$
- - - - $\alpha_{(u_T=0.4)}(270^\circ) = 16^\circ$



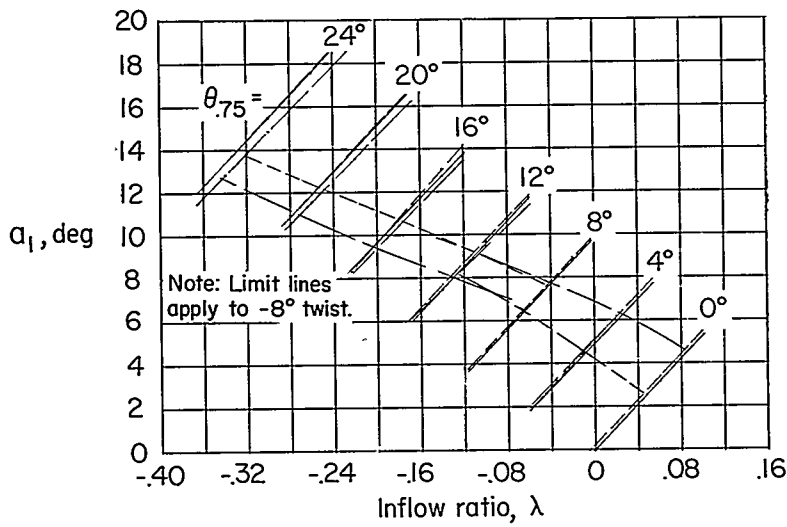
(e) $\mu = 0.30$.

Figure 1.- Continued.



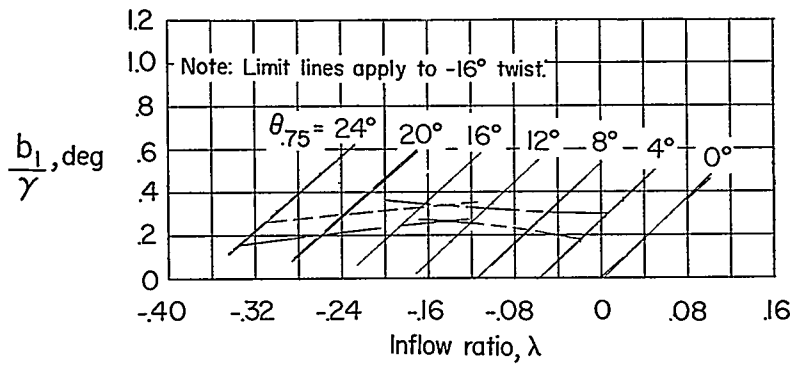
Flapping lines

- $\theta_1 = 0^\circ$
- $\theta_1 = -8^\circ$
- $\theta_1 = -16^\circ$



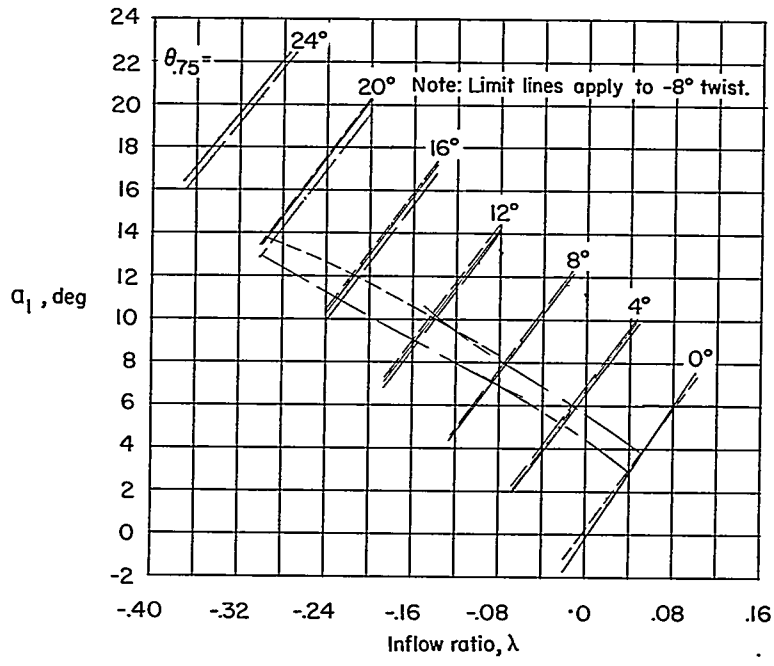
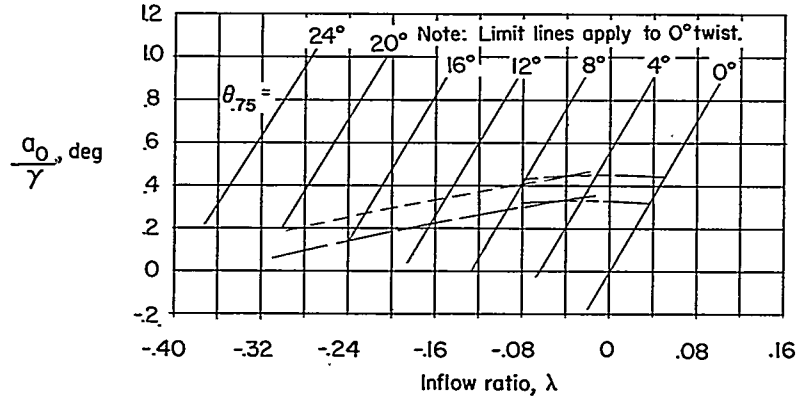
Limit lines

- $\alpha_{(1.0)(270^\circ)} = 12^\circ$
- $\alpha_{(u_T=0.4)(270^\circ)} = 12^\circ$
- $\alpha_{(1.0)(270^\circ)} = 16^\circ$
- $\alpha_{(u_T=0.4)(270^\circ)} = 16^\circ$

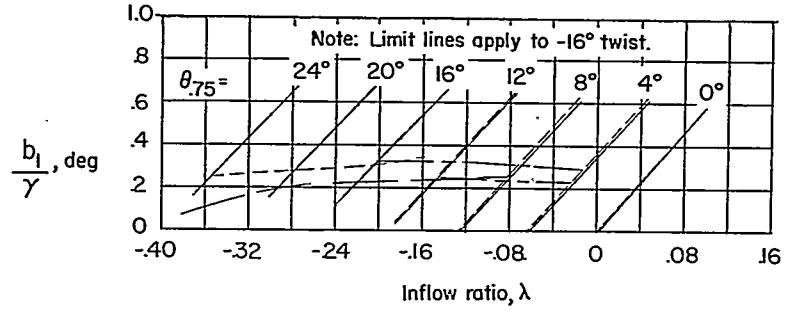


(f) $\mu = 0.40$.

Figure 1.- Continued.

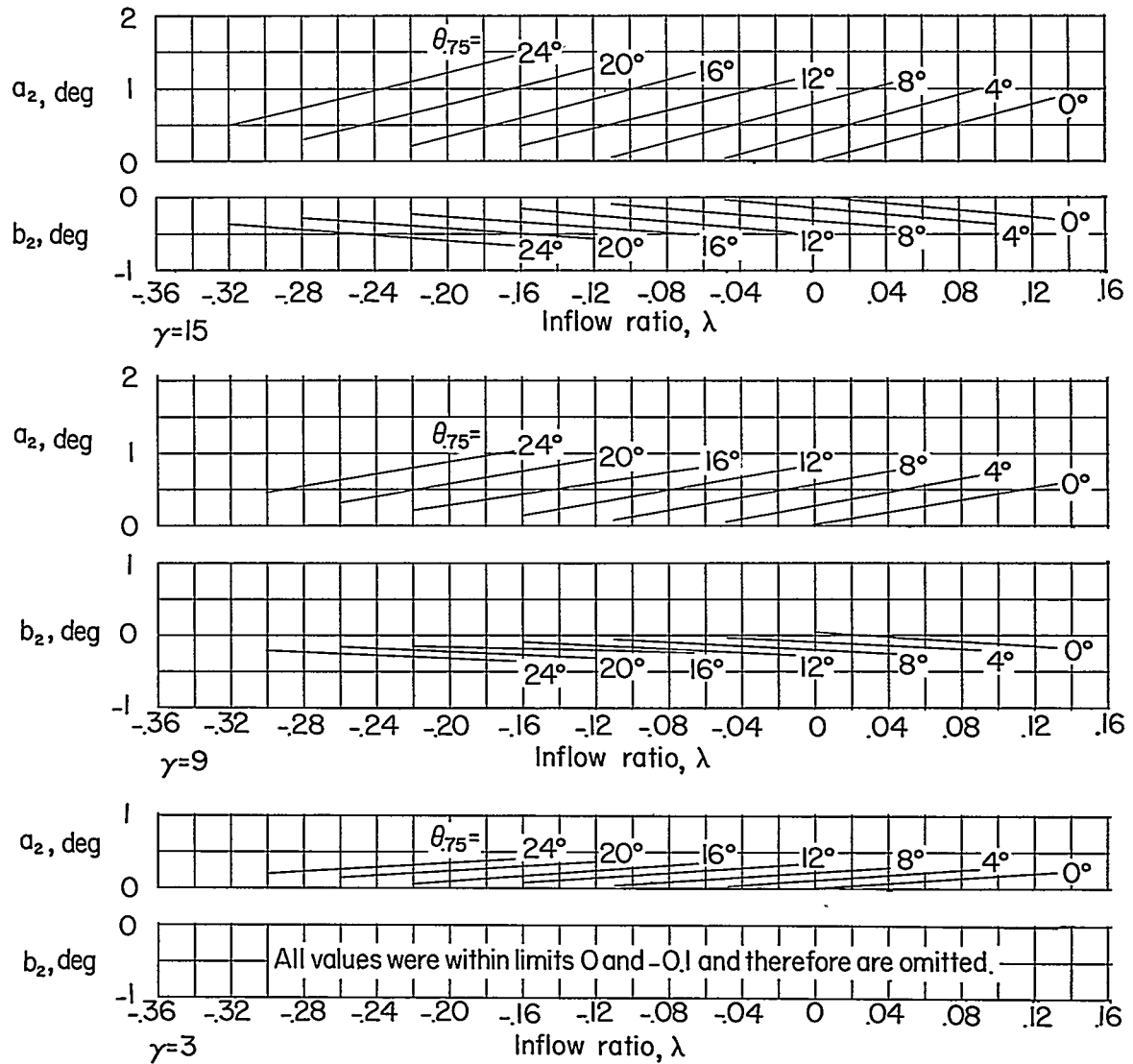


- Flapping lines
- $\theta_1 = 0^\circ$
 - - - $\theta_1 = -8^\circ$
 - - - $\theta_1 = -16^\circ$
- Limit lines
- $\alpha_{(10)(270^\circ)} = 12^\circ$
 - - - $\alpha_{(u_T=0.4)(270^\circ)} = 12^\circ$
 - - - $\alpha_{(10)(270^\circ)} = 16^\circ$
 - - - $\alpha_{(u_T=0.4)(270^\circ)} = 16^\circ$



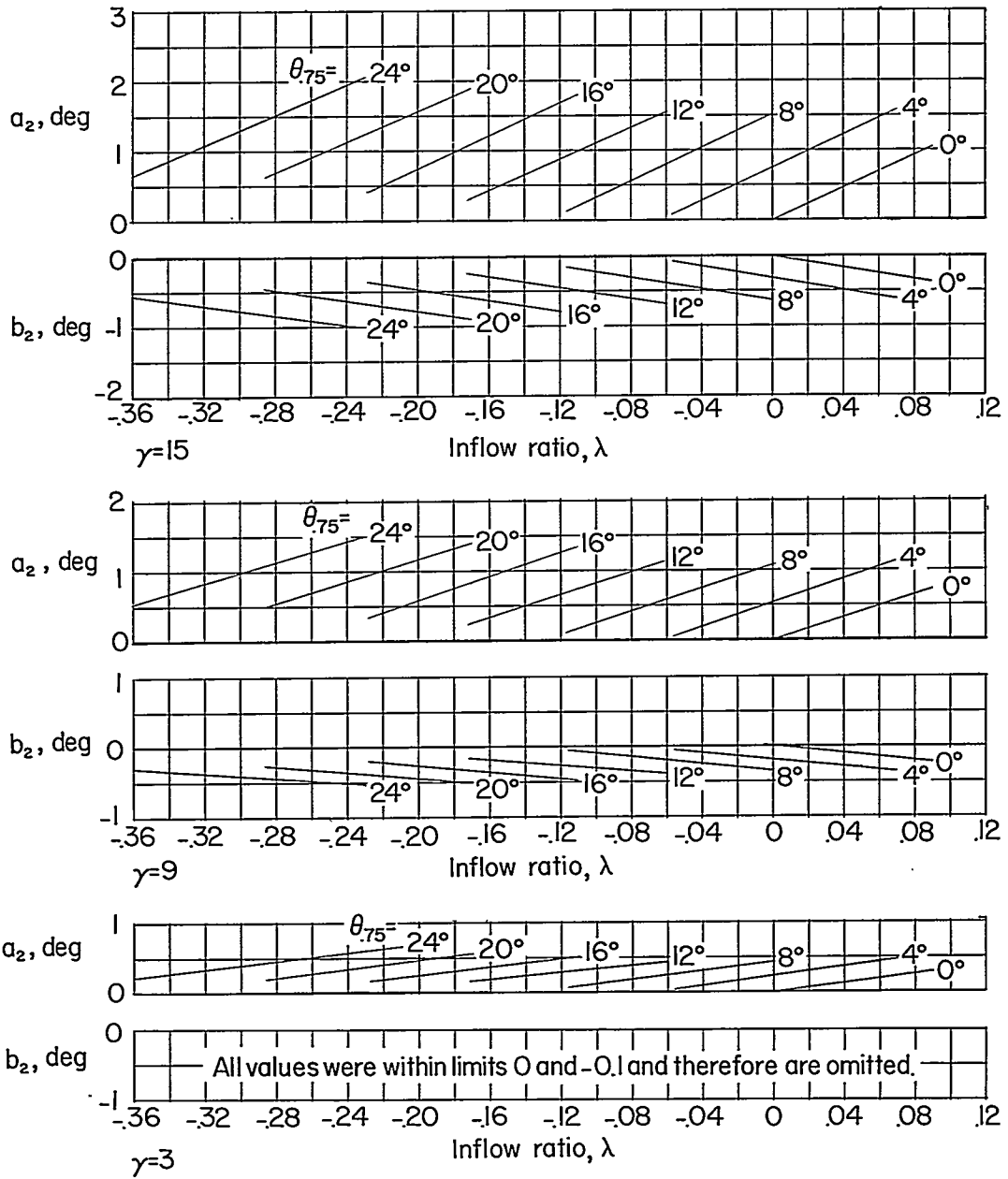
(g) $\mu = 0.50$.

Figure 1.- Concluded.



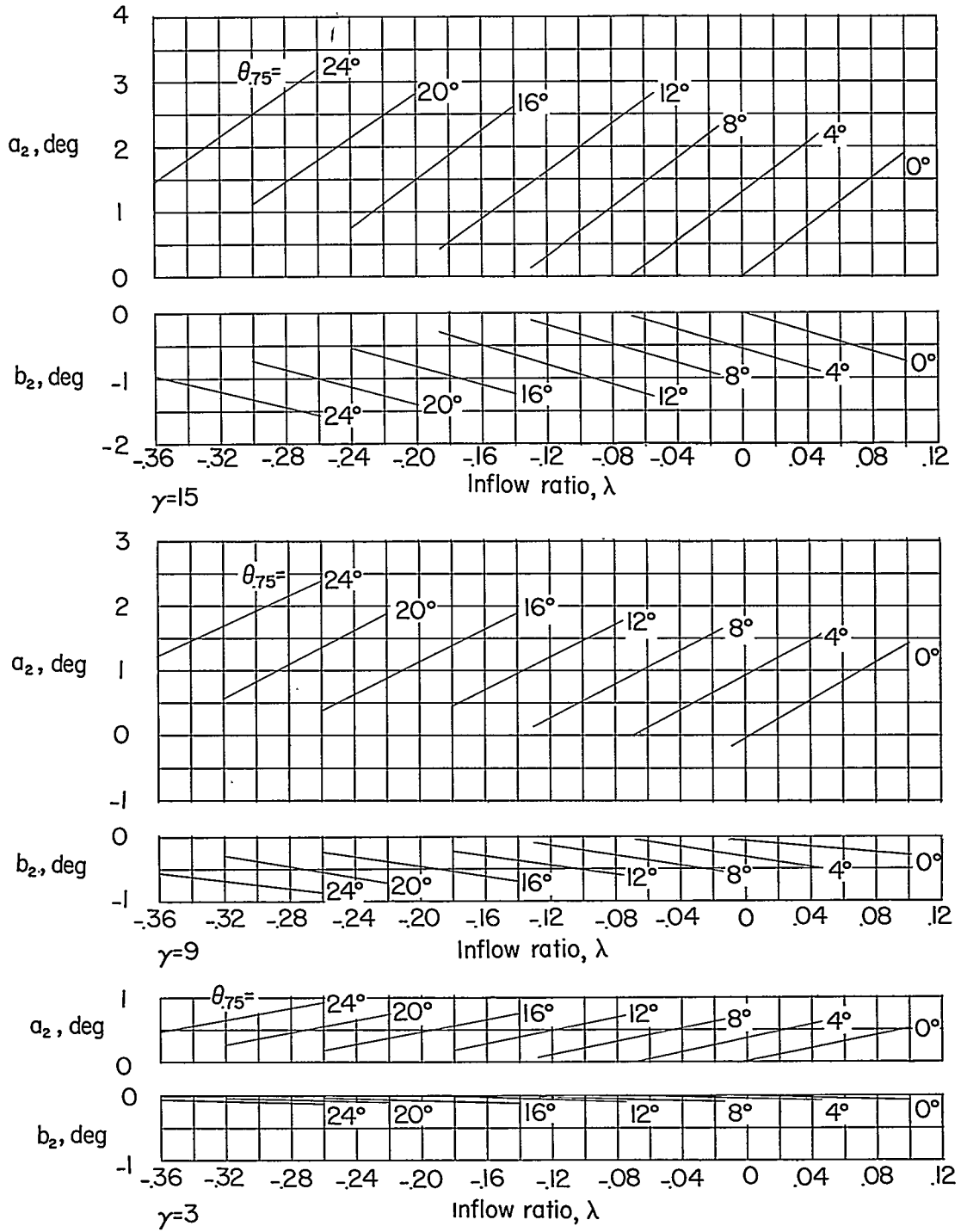
(a) $\mu = 0.30$.

Figure 2.- Second-harmonic flapping coefficients as a function of pitch angle and inflow ratio for blades having -8° twist.



(b) $\mu = 0.40$.

Figure 2.- Continued.



(c) $\mu = 0.50$.

Figure 2.- Concluded.